NAIC-ID(RS)T-0483-96

NATIONAL AIR INTELLIGENCE CENTER

IRRADIANCE OF SURFACE FIRE IN FORESTS

by

Chen Dawo, Wang Xiuqing, and Wei Chong

Approved for public release: distribution unlimited

HUMAN TRANSLATION

NAIC-ID(RS)T-0483-96 15 October 1996

MICROFICHE NR:

IRRADIANCE OF SURFACE FIRE IN FORESTS

By: Chen Dawo, Wang Xiuqing, and Wei Chong

English pages: 17

Source: Journal of Northeast Forestry University; pp. 32-40

Country of origin: China
Translated by: Leo Kanner Associates
F33657-88-D-2188
Requester: NAIC/DXDI/Erik Sondergelt
Approved for public release: Distribution unlimited.

GRAPHICS DISCLAIMER

All figures, graphics, tables, equations, etc. merged into this translation were extracted from the best quality copy available.

IRRADIANCE OF SURFACE FIRE IN FORESTS

Chen Dawo, Wang Xiuqing, and Wei Chong
Northeast Forestry University

ABSTRACT

This paper discussed the irradiance of fire lines to surface-ground while surface-ground spreading, and the effect of wind speed, slope on irradiance. The formula for calculation of irradiance of fire line to surface-ground was deduced by analysis to flame characteristics and by building up the radiation model of flame zone in fire line. The formula for calculating of irradiance of zone covered flame was deduced by taking the average height of flame as a unit of length and defining the spatial parameters of fire environment--ξ, η, ζ, its radiation field spatial characteristic function--$f(\xi, \eta, \zeta)$. Practical results revealed that the irradiance of fire line to surface-ground is related to flame temperature, fire intensity, flame average height, and the position of observation point. In addition, it is effected also by wind speed, slope. By compare, the irradiance of the sun to surface-ground is negligible during the short period of fire line approached to this area.
Key Words: Surface-ground fire; diffusion flame; radiation flux, solar constant.

Under field conditions, the combustible matter system in a forest is an open system. Fluctuations in water content in the

combustible matter is also a process of energy exchange and material exchange between combustible matter and environment. It is restricted by meteorological factors in nature (rainfall, wind, temperature, relative humidity and solar radiation, etc.) on the one hand, and by fire area spreading characteristics, on the other. Through convection and thermal radiation, a fire line transfers heat to its surrounding space and forms a high-temperature region in its adjacent area. During a short time while the fire line is spreading over scores of meters downwind, the latter plays a predominant part and causes the water content in the surface layer of the combustible matter to decrease rapidly. As far as the ground surface layer is concerned, thermal radiation plays a dominant role in the preheating process.

1. Thermal Radiation Model of Flame Zone in Fire Line

The flame of a surface fire is a diffusion flame. The thermal radiation characteristics of the flame zone in the fire line refer to the surface temperature of flame, surface area of the flame zone, and surface radiation character of the flame zone[1].

It is generally believed that the ignition temperature of a combustible gas mixture is much the same as its critical extinguishing temperature. But the actual situation is that a flame is extinguished when its temperature is still far higher than its ignition temperature. This kind of phenomenon is referred to as the ignition and extinguishing lag phenomenon[2]. Subsequently, the temperature in the flame zone should be higher than the ignition temperature. Table 1 lists the ignition temperatures of several combustible gas mixtures.

TABLE 1. Ignition Temperatures of Several Kinds of Matter[1]

t/℃

1 着火温度	2 木炭C	3 氢气H_2	4 一氧化碳CO	5 甲烷CH_4	6 乙烷C_2H_6	7 乙烯C_2H_4
空气中燃烧8	350	580～590	644～658	650～750	520～630	542～547
氧气中燃烧9		580～590	637～658	556～700	520～630	500～519

KEY: 1 - ignition temperature 2 - charcoal 3 - hydrogen 4 - carbon monoxide 5 - methane 6 - ethane 7 - ethylene 8 - burning in air 9 - burning in oxygen

As shown in Fig. 1, the length and front-edge width of a randomly selected small segment of a fire line are denoted with l and D. The spatial model of a flame zone in the fire line is converted into a recumbent triangular column, with A, B and C faces as the face sources for thermal radiation. They evenly dissipate radiant energy in every possible transfer direction, with dA as an area element randomly selected on the face source, dQ as the radiant heat emitted by area element dA in time dt, and M as irradiance ($W \cdot m^{-2}$).

$$M=dQ/dAdt \tag{1}$$

If the radiant-properties model of the flame zone is converted into graybody radiation, the irradiance of the face source will be given by the formula

$$M=e\sigma T^4$$

where T is the temperature of the face source (K); e is emissivity, whose transfer value, between 0 and 1, is determined by the surface properties of the face source: for the orange-red flame surface, e is approximately 0.93[3]; and σ is Stefan's constant.

2. Irradiance of Fire line with Respect to the Surface

As shown in Fig. 2, the space above the surface combustible layer is divided by the flame zone in the fire line into three

subspaces: I, II and III. Subspace I can be used to study

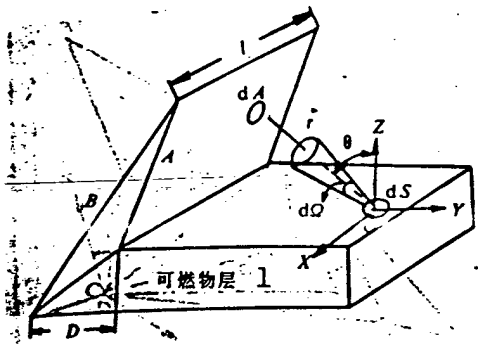

Fig. 1. Radiation model of flame zone in fire line
KEY: 1 - combustible layer

the irradiance received by the surface combustible matter during the preheating stage; subspace II serves in studying the irradiance received by tree crowns at the top of the fire line in its spreading process, while subspace III is employed in studying the irradiance received by the ground surface in the residual fire area.

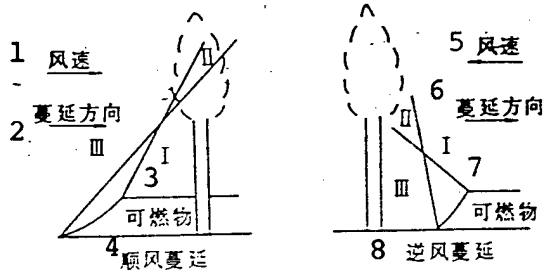

Fig. 2. Radiation area provided by fire line
KEY: 1 - wind speed 2 - direction of spreading 3 - combustible matter 4 - downwind spreading 5 - wind speed 6 - direction of spread 7 - combustible matter 8 - upwind spreading

The temperature at the face source is nonuniformly distributed and varies with time, i.e., $T=T(x,y,z,t)$. The face

source evenly distributes the radiant energy over a 2π solid angle. The energy radiated to solid angle $d\Omega$ from each unit area of the face source per unit time can be expressed as $(M/2\pi)d\Omega$. The radiant energy transmitted within the solid angle and reaching an area element per unit time ds is

$$(M/2\pi)d\Omega\cos\theta ds$$

As shown in Fig. 1, angle θ is an included angle between the transfer direction and the direction normal to area element ds. By integrating various transfer directions, the total radiant energy arriving at area unit ds per unit time can be found. Obviously, the total radiant energy is provided by the face source A, which is numerically equivalent to $d\Phi$, the radiation flux received by the area element ds:

$$d\Phi = (\int \frac{M}{2\pi}\cos\theta d\Omega)ds$$

By substituting Eq. (1) in the above formula and using E to represent the irradiance of the fire line with respect to the surface ($W \cdot m^{-2}$), we have

$$E = \frac{d\Phi}{dS} = \frac{e\sigma}{2\pi}\int T^4(x,y,z,t)\cos\theta d\Omega \qquad (2)$$

where the integration interval is the solid angle corresponding to face source A. As shown in Fig. 3, a spherical coordinate system is adopted with its point of origin placed at the investigated ds, where the OCD plane divides face source A (AA'F'F) into A_1 (CDA'F') and A_2 (CDAF). Let us first study the irradiance of the A_1 sub-face source to the surface and denote it as E_1.

As shown in Fig. 4, two surveyor poles of the same height are erected on the ground. Pole CD' is near the original point, while the other pole GB' is far from the original point. It can be seen from the Figure that $\gamma>\gamma_o$, $\theta>\theta_o$. If triangle OGB' is

rotated by the angle φ($\angle D'OB'$) counter-clockwise, then the space locations of triangle OCD′ and triangle OGB′ are precisely the

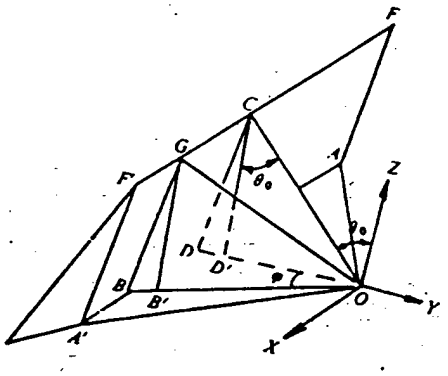

Fig. 3. Relationship among various quantities

triangles given in Fig. 3. By referring to Figs. 3 and 4 at the same time, $\theta=\angle ZOG=\angle OGB'$; the farther away from the original point the GB′ location is, the greater the values of γ,φ,θ can be; when GB′ is on the point at infinity, $\gamma\to\infty$, $\varphi\to\pi/2$. Obviously, there are constraining conditions among γ,φ,θ (see Fig. 3),

$$\cos^2\theta=GB'^2/OG^2=GB'^2/(OC^2+GC^2)$$

Since $GC^2=B'D'^2=(OD'\,tg\varphi)^2$, and $OD'^2=OC^2-CD'^2=OC^2-GB'^2$, then

$$\cos^2\theta=\frac{GB'^2}{OC^2+(OC^2-GB'^2)tg^2\varphi}=\frac{GB'^2}{OC^2}\frac{1}{1+tg^2\varphi}\frac{1}{\left[1-\frac{GB'^2}{OC^2}tg^2\varphi/(1+tg^2\varphi)\right]}$$

Let us write $GB'=H$, $OC=r_0$, and note that $(1+tg^2\varphi)^{-1}=\cos^2\varphi$, then

$$\cos^2\theta=(\frac{H}{r_0}\cos\varphi)^2/[1-(\frac{H}{r_0}\sin\varphi)^2]$$

and as $H\le r_0$, $0\le\varphi<\pi/2$, constantly $(H/r_0\sin\varphi<1$. Therefore,

$$1/[1-(\frac{H}{r_0}\sin\varphi)^2]=1+(\frac{H}{r_0}\sin\varphi)^2+(\frac{H}{r_0}\sin\varphi)^4+(\frac{H}{r_0}\sin\varphi)^6+\cdots$$

Let

$$1/[1-(\frac{H}{r_0}\sin\varphi)^2]\approx 1+(\frac{H}{r_0}\sin\varphi)^2+(\frac{H}{r_0}\sin\varphi)^4+(\frac{H}{r_0}\sin\varphi)^6$$

then:

$$\cos^2\theta \approx (\frac{H}{r_0}\cos\varphi)^2[1 + (\frac{H}{r_0}\sin\varphi)^2 + (\frac{H}{r_0}\sin\varphi)^4 + (\frac{H}{r_0}\sin\varphi)^6] \tag{3}$$

If the temperature at the A_1 sub-face source is rewritten as $T(\gamma,\varphi,\theta,t)$, $d\Omega=\sin\theta d\theta d\varphi$, the irradiance of the A_1 sub-face source with respect to the investigation site is

$$E_1 = \frac{e\sigma}{2\pi}\int_0^{\varphi} d\varphi \int_0^{\theta} T(r,\varphi,\theta,t)\sin\theta\cos\theta d\theta \tag{4}$$

Eq. (4) provides a method of calculating E_1, where flame height H (implicitly contained in $\cos\theta$) and flame surface temperature T are both parameters, which basically are restricted by four factors, namely wind speed, type of combustible matter, load of combustible matter, and water content of combustible matter. If the surface combustible layer has a uniform distribution and the same combustion character, then the $\overline{H}$ and $\overline{T}$ values vary only with wind speed. If the wind speed is divided into several intervals and a mean value of the corresponding flame height and temperature is selected from various intervals and marked with and $\overline{T}_i$ $(i=0,1,2,\ldots,n)$, then the following can be derived from $\overline{H}_i$ Eq. (4):

$$E_1 \approx \frac{e\sigma}{8\pi}\overline{T}_i^4\{\frac{\overline{H}_i^2}{r_0^2}[\varphi_1 + \frac{1}{2}\sin 2\varphi_1] + \frac{\overline{H}_i^4}{4r_0^4}[\varphi_1 + \frac{1}{2}\sin 2\varphi_1(2\sin^2\varphi_1 - 1)]$$
$$+ \frac{\overline{H}_i^6}{6r_0^6}[\varphi_1 + \frac{1}{2}\sin 2\varphi_1(2\sin^4\varphi_1 - 1)] + \frac{\overline{H}_i^8}{8r_0^8}[\varphi_1 + \frac{1}{2}\sin 2\varphi_1(2\sin^6\varphi_1 - 1)]\}$$

Similarly, the irradiance at the A_2 sub-face source with respect to the surface can also be calculated and expressed as E_2.

$$E_2 \approx \frac{e\sigma}{8\pi}\overline{T}_i^4\{\frac{\overline{H}_i^2}{r_0^2}[\varphi_2 + \frac{1}{2}\sin 2\varphi_2] + \frac{\overline{H}_i^4}{4r_0^4}[\varphi_2 + \frac{1}{2}\sin 2\varphi_2(2\sin^2\varphi_2 - 1)] + \frac{\overline{H}_i^6}{6r_0^6}[\varphi_2 + \frac{1}{2}\sin 2\varphi_2$$
$$(2\sin^4\varphi_2 - 1)] + \frac{\overline{H}_i^8}{8r_0^8}[\varphi_2 + \frac{1}{2}\sin 2\varphi_2(2\sin^6\varphi_2 - 1)]\}$$

where $\varphi_1=\angle D'OA'$, $\varphi_2=\angle D'OA$. Evidently, the irradiance at face source A with respect to the surface $E=E_1+E_2$, and we have the

expressions

$$E \approx \frac{e\sigma}{8\pi}\overline{T}_i^4\{\frac{\overline{H}_i^2}{r_0^2}[\varphi_1+\varphi_2+\frac{1}{2}(\sin 2\varphi_1+\sin 2\varphi_2)]$$
$$+\frac{\overline{H}_i^4}{4r_0^4}[\varphi_1+\varphi_2+\frac{1}{2}\sin 2\varphi_1(2\sin^2\varphi_1-1)+$$
$$\frac{1}{2}\sin 2\varphi_2(2\sin^2\varphi_2-1)]+\frac{\overline{H}_i^6}{6r_0^6}[\varphi_1+\varphi_2+$$
$$\frac{1}{2}\sin 2\varphi_1(2\sin^4\varphi_1-1)+\frac{1}{2}\sin 2\varphi_2(2\sin^4\varphi_2-1)]+$$
$$\frac{\overline{H}_i^8}{8r_0^8}[\varphi_1+\varphi_2+\frac{1}{2}\sin 2\varphi_1(2\sin^6\varphi_1-1)+\frac{1}{2}\sin 2\varphi_2(2\sin^6\varphi_2-1)]\}$$

By rearrangement, the precise value of irradiance is given by the expression

$$E=\frac{e\sigma}{4\pi}\overline{T}_i^4\frac{\overline{H}_i^2}{r_0^2}\{(\varphi_1+\varphi_2)(\frac{1}{2}+\frac{\overline{H}_i^2}{8r_0^2}+\frac{\overline{H}_i^4}{12r_0^4}+\frac{\overline{H}_i^6}{16r_0^6}-\cdots)+\frac{1}{2}\sin 2\varphi_1[(\frac{1}{2}$$
$$+\frac{\overline{H}_i^2}{4r_0^2}\sin^2\varphi_1+\frac{\overline{H}_i^4}{6r_0^4}\sin^4\varphi_1+\frac{\overline{H}_i^6}{8r_0^6}\sin^6\varphi_1+\cdots)-(\frac{\overline{H}_i^2}{8r_0^2}+\frac{\overline{H}_i^4}{12r_0^4}+\frac{\overline{H}_i^6}{16r_0^6}+\cdots)]$$
$$+\frac{1}{2}\sin 2\varphi_2[(\frac{1}{2}+\frac{\overline{H}_i^2}{4r_0^2}\sin^2\varphi_2+\frac{\overline{H}_i^4}{6r_0^4}\sin^4\varphi_2+\frac{\overline{H}_i^6}{8r_0^6}\sin^6\varphi_2+\cdots)-(\frac{\overline{H}_i^2}{8r_0^2}+\frac{\overline{H}_i^4}{12r_0^4}+\frac{\overline{H}_i^6}{16r_0^6}+\cdots)]$$

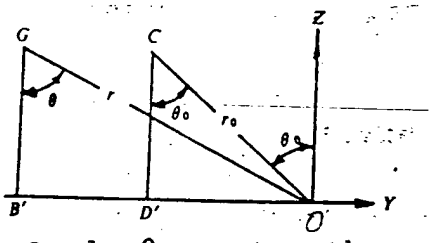

Fig. 4. Angle θ greater than angle θ_0

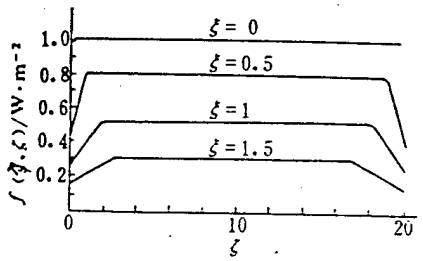

Fig. 5. $f(\xi,\zeta)$ values at different points of ground surface within fire environment when $l = 20\overline{H}_i$

In actual forest fires, flame height and temperature are extremely diversified and are measured through actual measurements. Since wind speed and the distribution of combustible matter vary randomly, flame heights measured by erecting surveyor's poles are far from accurate. On the other hand, flame temperatures measured using a special thermocouple are also extremely inaccurate due to radiant heat dissipation, convective heat transfer, and thermal inertia. The errors occurring in actual measurements are much greater than those derived from approximate calculations. Therefore,

$$E \approx \frac{e\sigma}{4\pi}\overline{T}_i^4 \frac{\overline{H}_i^2}{r_0^2}(\varphi_1 + \varphi_2 + \frac{1}{2}\sin 2\varphi_1 + \frac{1}{2}\sin 2\varphi_2) \tag{5}$$

It can be concluded from Eq. (5) that: (1) The surface irradiance provided by the fire line is directly proportional to the fourth power of the average flame surface temperature.
Let $E_0(\overline{T}_i) = e\sigma\overline{T}_i^4/4$, which describes only the graybody radiation properties of the face source. $\overline{T}i$ is based on the Kelvin temperature standard. Calculations indicate that $E_0(1237) \approx 2E_0(1073)$, $E_0(1773) \approx 7.5E_0(1073)$.

(2) The irradiance of the fire line with respect to the surface is directly proportional to the square of the average flame height. At the i-th level wind speed, if the average flame length, flame dip, and fire intensity are respectively expressed as $\overline{L}_i$, α_{i0} and I_i, then

$$\overline{L}_i = 0.077\,5I^{0.46}[4] \qquad \overline{H}_i^2 = 6.01 \times 10^{-3} I_i^{0.92}\sin^2\alpha_{i_0}$$

or using an approximate computing formula

$$\overline{H}_i^2 \approx 4\text{x}10^{-3}\text{I}_i\,[5]$$

By substituting it in Eq. (5),

$$E = 6.01 \times 10^{-3} I_i^{0.92}\sin^2\alpha_{i0} E_0(\overline{T}_i)(\varphi_1 + \varphi_2 + \frac{1}{2}\sin 2\varphi_1 + \frac{1}{2}\sin 2\varphi_2)/r_0^2$$

$$E \approx 4 \times 10^{-3} I_i E_0(\bar{T}_i)(\varphi_1 + \varphi_2 + \frac{1}{2}\sin 2\varphi_1 + \frac{1}{2}\sin 2\varphi_2)/r_0^2$$

(3) The irradiance of the fire line with respect to the surface is inversely proportional to the square of r_0, the distance between the investigation site, and the flare. When the investigation site is right under the flare as shown in Fig. 3, point O and point D' will coincide. At this instant, r_0 reaches its minimum value and $r_0 = \bar{H}_i$.

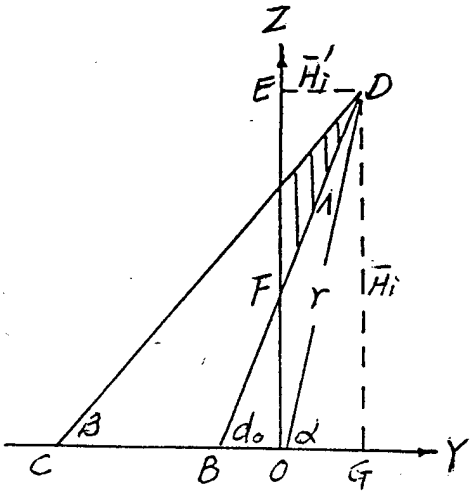

Fig. 6. Investigation site within flame-covered zone

The irradiance in the fire environment is estimated using the average flame height as unit length. Eq. (5) can be rewritten as

$$E = E_0(\bar{T}_i)(\varphi_1 + \varphi_2 + \frac{s_0 l_1}{s_1^2} + \frac{s_0 l_2}{s_2^2})/\pi(1 + \frac{s_0^2}{\bar{H}_i^2}) \qquad (6)$$

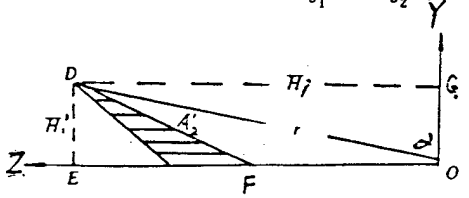

Fig. 7. Irradiance of A_2 face source with respect to point O

As shown in Fig. 3, in the above equation, s_0=OD′, s_1=OA′, s_2=OA′, l_1=CF′, l_2=CF, $l=l_1+l_2$=FF′ and are estimated by using the denominator in Eq. (6). When the investigation site is right under the flare, $s_0=0$, and the denominator is π; when $s_0=10\overline{H}_i$, the denominator increases to 101π, and its surface irradiance decreases to several thousandths under the flare and can be neglected. The fire intensity is smaller than the 3000 and 100kw/m mid- to low-intensity surface fires; their average flame length (L_i) is less than 3m and 1.8m respectively. It is known then that for mid- to low-intensity surface fires, the fire line irradiance to the surface can be calculated starting from 30m. During surface fire stable spreading, the length of fire line is much greater than the average flame height, i.e., $l \gg H_i$. Let

$$s_0 = \xi\overline{H}_i, \quad l = \eta\overline{H}_i, \quad l_1 = \zeta\overline{H}_i.$$

and substitute these expressions in Eq. (6),

$$E = E_0(\overline{T}_i)f(\xi,\eta,\zeta)$$

$$f(\xi,\eta,\zeta) = [\sin^{-1}\frac{\zeta}{\sqrt{\xi^2+\zeta^2}} + \sin^{-1}\frac{(\eta-\zeta)}{\sqrt{\xi^2+(\eta-\zeta)^2}} + \frac{\xi\zeta}{\xi^2+\zeta^2} + \frac{\xi(\eta-\zeta)}{\xi^2+(\eta-\zeta)^2}]/\pi(1+\xi^2) \quad . \tag{7}$$

where ξ,η,ζ are all nondimensional quantities, which can be used to evaluate the spatial dimension of a fire environment with the average flame height as unit length. The function $f(\xi,\eta,\zeta)$ is also a nondimensional quantity, with its maximum value 1 and minimum value 0, which expresses the spatial properties of the radiation field. Given the fire line length $\eta=20$ and the distance between the investigation site and fire line (ξ value) as a parametric variable, the f vs. ζ plot is shown in Fig. 5.

3. Irradiance Provided by Fire Line with Respect to Flame-covered Zone

It is known from Fig. 2 that during downwind spreading, the area from the fire line front-edge to somewhere right under the flare is a flame-covered zone, while during upwind spreading, the area from the flare after-edge to somewhere under the flare is the flame-covered zone. The flame-covered zone is characterized by a unique evaluation of spatial parameters ξ,ζ,η in the fire environment, which leads to a special evaluation of the spatial properties function $f(\xi,\eta,\zeta)$ of the radiation field. When the investigation site is right under the flare, $s_0=0$ and therefore, $\xi_1=0$. If the investigation site is not located at the end point, then $\zeta_1=l_1/\overline{H}_i\neq 0$、 $\eta_1-\zeta_1=(l-l_1)/\overline{H}_i\neq 0$. From Eq. (7),

$$f(\xi_1,\eta_1,\zeta_1)=1 \quad , \quad E_s=E_0(\overline{T}_i) \tag{8}$$

where E_s is the irradiance that the fire line provides with respect to the surface right under the flare, which is related to the temperature of the thermal radiation source alone, and is related neither to the average flame height nor to the fire line length.

As shown in Fig. 6, if the investigation site is located in the covered zone, face source A (denoted with DB) can be divided into two sub-face sources: A'_1 (denoted with BF) and A'_2 (denoted with DF). Their irradiance to the surface can be expressed with E', E'_1 and E'_2. Since the investigation site is located right under the flare of the A'_1 sub-face source, the following can be derived from Eq. (8):

$$E'_1=E_0(\overline{T}_i)=\frac{e\sigma\overline{T}_i^4}{4}$$

Rotating the image in the hatched area in Fig. 6 by 90^0 counter-clockwise, Fig. 7 can be obtained. The effective flame height of sub-face source A'_2 is expressed with $\overline{H'}$; the length of the fire line corresponding to sub-face source A'_2, is equal to the length of the fire line corresponding to face source A; the distance $\overline{OE}$ between the investigation site and right under the flare of sub-face source A'_2 is equal to the average flame height

$\bar{H}_i$ of sub-face source A. Thus, the spatial parameters ξ_2, η_2, ζ_2 in the fire environment of sub-face source A'_2, respectively, are

$$\xi_2 = \frac{\bar{H}_i}{H'_i} \quad , \quad \eta_2 = \frac{l}{H'_i} \quad , \quad \zeta_2 = \frac{l_i}{H'_i} \quad .$$

During stable spreading of the fire line, l is constantly $l > \bar{H}_i$; if the investigation site is located in the central part of the flame covered zone, i.e., $l_1 > \bar{H}_i$ and $l - l_1 > \bar{H}_i$, then

$$\zeta_2 \gg \xi_2, \eta_2 - \zeta_2 \gg \xi_2 \quad .$$

From Eq. (7), the following is derived

$$f(\xi_2, \eta_2, \zeta_2) = \frac{1}{1 + \xi_2^2} \quad , \qquad E'_2 = E_0(T_i)/(1 + \xi_2^2) \quad . \tag{9}$$

From Fig. 6, $\cos^2\alpha = (1 + \xi_2^2)^{-1}$. It is clear that the surface irradiance at face source A provides with respect to the flame-covered zone $E' = E'_1 + E'_2$. Therefore,

$$E' = \frac{e\sigma T_i^4}{4}(1 + \cos^2\alpha) \tag{10}$$

Let the flame dip be α_0, then in the flame covered zone, $\alpha_0 \leq \alpha \leq \pi/2$. The following can be concluded from Eq. (10):

(1) The surface irradiance that the fire line provides with respect to the flame-covered zone is greater than that in the non-flame-covered zone. In the flame-covered zone, as the investigation site approaches the front-edge of the fire line, angle α decreases and the surface irradiance at the investigation site increases. Since the minimum value of α is the flame dip α_0, clearly $\alpha_0 \approx \beta$ (see Fig. 6). Thus, the irradiance at the front-edge of the fire line reaches its maximum value, and $E'_{max} = E_0(T_i)(1 + \cos^2\alpha_0) \approx E_0(T_i)(1 + \cos^2\beta)$.

(2) The maximum irradiance that the fire line provides with respect to the surface is associated not only with the temperature of the radiant source, but also with the flame dip. Under the same conditions of terrain, type, and load and water content of combustible matter, an increase in wind speed causes a decrease in flame dip and an increase in E'_{max}. Under the same

conditions of wind speed, type, and load and water content of combustible matter, an increase in the topographic slope angle will lead to a decrease in flame dip, and an increase in E'_{max}, as well.

(3) During surface fire spreading, the front edge of the downwind fire line is located at B in the flame-covered zone, while the front edge of the upwind fire line is located at C in the non-flame-covered zone. In these two situations, the radiant heat provided by the fire line differs greatly in quantity. This difference can be calculated with irradiance as the standard. The irradiance at B of the front edge of the downwind fire line is denoted with E_b, which can be calculated from Eq. (10)

$$E_b = E'_{max} = E_0(\overline{T}_i)(1 + \cos^2\alpha_0) \approx E_0(\overline{T}_i)(1 + \cos^2\beta)$$

Referring to Fig. 6, the distance between the front edge of the upwind fire line and right under the flare CG can also satisfy the condition $1 > \overline{CG}$, and the irradiance at C of the front edge of the upwind fire line is expressed with E_c, which can be calculated by using Eq. (9):

$$E_c = E_{max} = E_0(\overline{T}_i)/(1 + \xi^2) = E_0(\overline{T}_i)\sin^2\beta$$

where $\xi = \overline{CG}/\overline{H}_i$. Obviously, when wind speed or slope angle increases, angle α decreases, E_b increases, and then the fire condition of the downwind fire line will increase; when angle β decreases, E_c decreases, and then the fire condition of the upwind fire line will decrease.

(4) The irradiance of the sun is referred to as the solar constant, which is approximately 1.35kw/m^2, denoted with E_{so}. When sunlight passes through the atmosphere and arrives at the ground surface, its energy is approximately 31% of what it formerly was. Solar irradiance with respect to the surface is denoted with E'_{so}, and we have the expression

$$E'_{so}=0.31E_{so}(\sin\Phi\sin\delta+\cos\Phi\cos\delta\cos\gamma) \qquad (11)$$

where Φ is the latitude angle (^{0}) of the region where the solar

irradiance is under study (in ^{0}); δ is solar dip (^{0}); and γ is solar azimuth angle (^{0}).

As an example, let us consider Da Hinggan Ling Pr., where $\Phi \approx 48^0$, $\delta \approx 15^0$, noon time $\gamma=0$. By substituting these values in Eq. (11), $E'_{so}=0.35 kw/m^2$. Select $\bar{t}=900℃$, i.e., $\bar{T}=1\,173\ K$ is the average surface temperature of flame, which is then substituted into $E_0(\bar{T})=\varepsilon\sigma\bar{T}^4/4$, and the values $E_0=25.0 kw/m^2$ and $E'_{so}/E_0 \approx 1.4\%$ are obtained. It is therefore believed that during the short time that a fire line spreads over a distance of $10\bar{H}$, the solar irradiance with respect to the surface can be neglected.

4. Conclusions

The irradiance that the flame zone in the fire line provides with respect to the surface cannot be neglected. During the short period of time when the fire line spreads over scores of meters, the water content in the adjacent combustible surface layer rapidly decreases. It is possible to calculate quantitatively the radiant heat that $1m^2$ of surface receives in every second, and to determine its relationship with the characteristic value of the fire environment.

4.1. The irradiance that the fire line provides with respect to the surface is inversely proportional to the square of the distance between the investigation site and the flare.

4.2 The irradiance that the fire line provides with respect to the surface layer is directly proportional to the square of the average flame height and also is approximately directly proportional to fire intensity.

4.3 In judging the distance from the fire line length, from the investigation site to the flare, a general law can be derived

by using flame height as unit length.

4.4 The maximum irradiance of the downwind spreading of a surface fire E'_{max} is much greater than that of the upwind spreading surface fire E_{max}.

$$E'_{max} = E_0(\bar{T}_i)(1 + \cos^2\alpha_0) \approx E_0(\bar{T}_i)(1 + \cos^2\beta)$$

$$E_{max} = E_0(\bar{T}_i)\sin^2\beta$$

The angle β decreases with increase in wind speed and in slope angle.

REFERENCES

1. Guo Bowei et al. Smelting Furnace Fuel and Its Combustion, China Industry Publishing House, 1962.

2. Zhang Binquan, Fundamentals of Combustion Theory, Beijing Aeronautics and Astronautics University Publishing House, 1990.

3. R.B. Berde et al. Transfer Phenomena, Beijing Chemical Industry Publishing House, 1990.

4. Ju Ende and Chen Dawo, "Quantitative calculations of characteristic volume of Surface fire behavior." J. Northeast For. Univ., Vol. 3, No.2, Nov. 1992.

5. Wang Zhengfei, "Universal forest fire-insurance level system," Natural Disasters Journal, 1992, 7(3).

6. Charlede (American), Forest Microclimate, Beijing Meteorology Publishing House, 1986.

This paper was received on January 13, 1993 (paper was edited by Guo Haiyan).